Teknomekanik, Vol. 8, No. 2, pp. 164-182, December 2025
e-ISSN: 2621-8720 p-ISSN: 2621-9980

Investigation of corrosion, hardness, and wear rate of rice husk-zinc composite coating on A36 steel using dual anode electrolytic deposition technique

Samuel A. Ajayi[1], Peter P. Ikubanni[1,*], Peter Onu[1], Timothy A. Adekanye[2], Abideen T. Oyewo[3] and Olufemi Ajide[3]

[1] Department of Mechatronics Engineering, College of Agriculture, Engineering and Science, Bowen University, **Nigeria**
[2] Department of Mechanical Engineering, College of Engineering, Landmark University, **Nigeria**
[3] Department of Mechanical Engineering, Faculty of Engineering, Osun State University, **Nigeria**
[4] Department of Mechanical Engineering, Faculty of Engineering, University of Ibadan, **Nigeria**

* Corresponding Author: peter.ikubanni@bowen.edu.ng
Received: 23 July 2025; *Revised:* 09 October 2025; *Accepted:* 20 October 2025

Cite this https://doi.org/10.24036/teknomekanik.v8i2.42172

Abstract: Zinc-bas ed composite coatings developed from synthetic ceramics (Si_3N_4, SiC, and Al_2O_3) have recently been employed as reinforcement to enhance their resistance to deterioration. However, there is limited literature on the utilization of ceramic particles sourced from agro-industrial wastes in the formulation of these coatings. This study investigated the effect of the surface improvement process (SIP) using rice husk (RH) nanoparticles on the hardness and wear rate of A36 steel. The A36 steel, zinc bar, and RH nanoparticles were procured and characterized using Energy Dispersive Spectroscopy (EDS). Four cathode specimens were produced, including an as-received specimen of A36 steel and two anodes of zinc. Four steel specimens coated with Zn-10RH(t25), Zn-10RH(t30), Zn-15RH(t25), and Zn-15RH(t30), denoted as S1, S2, S3, and S4, respectively, were developed with concentrations of 10 or 15 g/L and deposition times of 25 or 30 minutes at a constant cell voltage of 0.5 V. The as-received substrate steel was used as the control specimen (CS). The hardness and wear rate (WR) properties of the deposited samples were examined using Vickers hardness (HV) and a Pin-on-disc tribometer, respectively. All coated specimens exhibited substantial improvements in hardness and wear rate properties compared to CS (Hardness = 85.82±0.45 HV and WR = 2.45±0.34 g/min). For the coated specimens, the hardness and WR values ranged from 188.50 to 288.37 HV, 260.34 to 284.38 MPa, and 0.01 to 0.02 g/min, respectively. The inclusion of the coatings significantly enhanced the mechanical properties of the deposited specimens.

Keywords: electrodeposition; rice husk; zinc-base; composite coatings; A36 steel

1. Introduction

The electrolytic deposition coating is a unique method among the various coating deposition techniques in material engineering research for surface modification of materials. It serves as an outstanding technique due to its uniformity in coating production, ease of control, and cost-effectiveness [1], [2]. Material coating production significantly enhances mechanical properties, including impact resistance, fatigue strength, hardness, wear resistance, and corrosion resistance [3], [4]. The dual anode electrolytic deposition technique is a distinctive electrochemical process central to research aimed at improving current circulation through the addition of particles in metal matrix composites (MMC) and providing better control for enhanced effectiveness and uniformity in coatings [5], [6]. This dual anode electrolytic technique consists of two anodes in an electrolytic cell, which affects the rate of deposition, uniformity in the electrochemical process, and current

distribution used for material purification, electrochemical studies, and corrosion processes [7], [8]. Zinc materials are utilized as coatings on low-carbon steels, such as A36 steel, to improve corrosion performance, surface hardness, and antioxidant protection [9]. However, when the material is subjected to abrasive applications, pure zinc coating is unsuitable due to its low hardness and tendency to scratch easily, leading to minimal wear resistance [10], [11]. The coating performance can be enhanced by incorporating hard, inert particles such as rice husks to transform the coating into a valuable zinc-based metal matrix composite (MMC).

Agricultural wastes, utilized as reinforcement particle composite materials for coatings, are gaining attention in research due to their cost-effectiveness, resource recycling, and support for sustainable goals. Several studies have reported the influence of agro-waste on engineering applications [12-14]. The corrosion behavior of a nickel surface-deposited Al MMC reinforced with bamboo leaf ash was studied. It was noted that the Ni-deposited Al-BLA composite enhanced corrosion resistance and improved mechanical behavior as reinforcement percentages increased [15]. The inclusion of rice husks, a byproduct of agro-waste, in the MMC, like zinc, enhances the mechanical properties and wear resistance of the material due to the presence of silica and other compounds [16-19].

The dual anode electrolytic deposition method improves homogeneous coating and integration of particles into matrix composites to achieve uniformity of current distribution and control of particle migration [15]. Some previous studies showed enhancement in the engineering properties of specimens coated via this method. Shi et al. [20] enhanced hydroxyl methylcellulose (HPMC) coatings with Al, Cu, Al_2O_3, and copper oxide nanoparticles on composite materials in tackling wear damage challenges. Hence, the additive composite coatings improved the load-bearing capacity and tribological behaviour of the cellulose-based composite coatings. The study revealed that metal oxide nano-fillers offered enhanced tribological properties compared to metal nanoparticles. To enhance the properties of mild steel, rice husk ash (RHA) particle was incorporated into electroless Ni-P coatings. The effect of the coatings at various concentrations of RHA particles was investigated on the deposition rate, surface morphology, and corrosion behaviour. The study revealed an increased deposition rate with increased RHA particles, with good bonding indication between the Ni-P matrix and RHA particles. The study showcased RHA particles as a cheaper and eco-friendly alternative for the improvement of the properties of the electroless Ni-P coatings [21].

The anti-wear and hardness values of the electrodeposited Zn-ZnO-xRHA composite coating were investigated with the deposition parameters of the RHA particulate loading were 0, 10, and 20 g at 15 min. deposition, 1.4 A current, 400 rpm stirring rate, and 75 °C bath temperature [22]. A chloride-based bath was employed for the deposition bath. The study revealed that the Zn-ZnO-20RHA-coated substrate possessed the highest hardness, while the wear loss of the developed composite coatings declined with increased RHA loading. In another study by Ajayi et al. [23], the combination of rice husk (RH) and white clay (WC) particulates was used to develop zinc-based composite coatings on A36 steel. The steel samples were coated with 10 and 15 RHWC particles. The study explored the effect of the coatings on the hardness, tensile strength, and wear rate properties of the samples, as well as microstructural examinations. The coated specimens revealed improved engineering properties over the uncoated samples of the A36 steel with Zn-13 RHWC using the dual-anode electrolyte co-deposition technique. Electrodeposition technique was employed to deposit pure zinc and its Zn-WO_3 (Zinc-Tungsten trioxide composite coatings on mild steel specimens. The influence of the WO_3 particles on Zn deposition, surface morphology of the composite, and the texture coefficient was analyzed. The specimen coated with Zn-WO_3 composites showed higher corrosion resistance and microhardness. The nanocomposite coatings successively protect the mild steel used from chemical or electrochemical disintegration in the subjected environmental conditions [24].

Limited literature on the use of ceramic particles of agro-industrial wastes for the enhancement of the engineering performance of metallic materials makes this study germane. More studies are required to be carried out on the utilization of agro-waste as a co-deposition coating material on metal substrates. Therefore, this study is aimed at using the dual anode electrolytic deposition technique for zinc composite coating, which is reinforced with rice husk agro-waste particles deposited on A36 steel. The mechanical and corrosion properties of the coated steel were investigated using appropriate protocols. The effects of the concentration of the rice husk particles and the duration of the deposition on the tribological performance, microhardness, and microstructural properties of the final coatings are investigated as the objectives of the study.

The research outcome is expected to enhance the sustainability of the composite coatings and excellent durability, especially for steel applications that require surface modification with cost-effectiveness. It is also likely to improve the utilization of agricultural wastes in the engineering field, which is one of the global sustainable development goals in the field of material research.

2. Material and methods

2.1 Material selection

A rectangular mild steel plate (ASTM A36) of dimensions 800 mm x 800 mm x 2 mm was sectioned. The saturated mild steel was the specimen used for this research. The steel plate used in this study was obtained commercially from a metal vendor in Iwo Road, Ibadan, Oyo State, Nigeria. Mild steel was chosen as it is readily available and is not expensive. It is one of the most globally used metals. Mild steel usage is exceptional, ranging from domestic to industrial applications. The choice of this metal over others is based on its wide range of applications, cheapness, and ease of accessibility. Figure 1 depicts the flow chart of the experimental procedure observed in this study.

2.2 Experimental design

The design of experiment used for the experimental setup was based on the Taguchi method using Minitab 19 software. Two controllable input parameters, namely, nanoparticle and deposition time, were considered for experimentation. Hence, for each parameter, two levels were presumed as shown in Table 1. For a two-factor-two-level experiment, Taguchi itemized an L_4 (2^2) orthogonal array for the experimental setup. Hence, a total of four experimental trials were used following the Taguchi L_4 orthogonal array of experimental design as shown in Table 2. Each nanoparticle evaluation was carried out on a new workpiece material, as shown in Table 3. Before actual electroplating, the rust layers were removed by polishing using emery cloth to minimize any effect of homogeneity on the experimental results. Other constant parameters that were used during the experiment are given in Table 4.

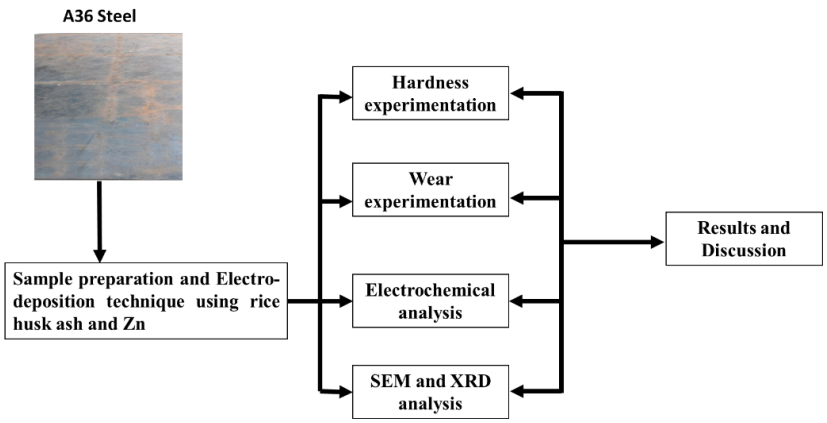

Figure 1. Schematic flowchart of the experimental procedure

Table 1. Controllable input parameters and their levels

Factors	Levels	
	Level 1	Level 2
Nano Particle (µm)	10	15
Deposition Time (Min.)	25	30

Table 2. Design of Experiment [Taguchi L_4 (2^2) Orthogonal Array]

Experimental Run	Input Parameters	
	Nano Particles (g/L)	Deposition Time (min)
1	10	25
2	10	30
3	15	25
4	15	30

Table 3. Chloride bath composition

Component	Quantity (g/L)
Zinc chloride (ZnCl)	130
Sodium chloride (NaCl)	50
Potassium chloride (KCl)	35
Boric acid	10
Thiourea	10
Glycine	10
RH	10/15

Table 4. Constant parameters considered

Parameter	Quantity
pH	4.5
Current density (A/cm^2)	2
Temperature (^{o}C)	45
Voltage (V)	0.5

2.3 Electrodeposition process

The choice of electro-deposition materials, such as metal alloys, ceramic composites, and biomaterials, was based on their individual physical and chemical properties. Pure zinc (with 99.9% zinc composite) was selected as an anode. It was chosen because of its excellent protective characteristics, ability to form strong covalent and stable bonds with other metal alloys, moderate reactivity, and strong reduction potential. Other composite materials were added to zinc to obtain durable protection, as zinc tarnishes on its own when it reacts with the atmospheric medium, and it will form flakes of oxide and carbonate. The electro-deposition composite material used for co-deposition in zinc electrolytes was rice husk (RH). RH nanoparticles (Figure 3) were chosen due to their sustainability and attractive mechanical, chemical, and physical properties. It possesses some essential features, which are: it is commonly available and affordable; ranked among the best non-toxic substances; and has a high content of silica, ranging from 90 to 97%. The bath formulation is the combination of the composite, which is the main material to be deposited, and other compounds that will help in facilitating the process. The composition of the bath was varied based on the applied method and the concentration of the reinforcement particles. The bath formulated for this work is a chloride bath. Electrodeposition was carried out by measuring each constituent in grams (g) using

an electrical analytical weighing balance (OHAUS Pioneer PA214) to get an accurate measurement. The bath constituents were put into a vessel and mixed with one liter of purified water. The content is then mixed vigorously and allowed to dissolve for 24 hours using a magnetic stirrer at 250 rpm. A typical electro-deposition process is displayed in Figure 2.

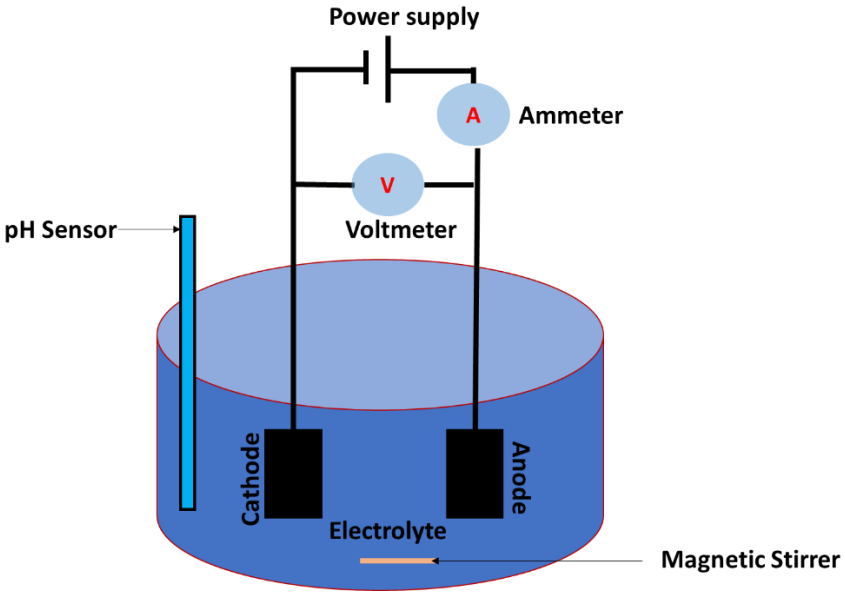

Figure 2. A typical electrodeposition process

2.4 Coating efficiency of RH deposited samples

The protective capability of the composite samples was further studied by calculating the coating efficiency of each of the thin film deposited specimens, with respect to the polarization resistance, using Equation 1.

$$Coating\ Efficiency\ (CE) = (1 - \frac{PR\theta_1}{PR\theta_2}) \times 100\% \quad (1)$$

where $PR\boldsymbol{\theta}_1$ is the polarization resistance of the control specimen, and $PR\boldsymbol{\theta}_2$ represents the respective coatings' polarization resistance.

2.5 Characterization of electrodeposited specimens

The morphologies and structures found in the deposited coatings were studied using the scanning electron microscope (SEM) technique. An energy-dispersive spectrometer (EDS) was used to determine the elemental composition and quantity. The phases of the electrodeposited specimen were obtained via a PANalytical Empyrean diffractometer. Rockwell hardness scale was utilized in this research for the assessment of the deposited samples and the control specimen (CS). The process provides a precise measurement of the exact hardness result required. Rockwell hardness testers employ a differential-depth approach to determine hardness. The test involves pressing an indenter into the material and then applying a slight load to establish the zero location. A heavy weight is introduced after the minor load and then removed while the nominal load is maintained. The depth difference between the nominal and main loads determines the hardness. All the coated specimens, as well as the control specimen, were subjected to a wear test using a pin-on-disc wear test to ensure their wear resistance when they come in contact with other materials in relative motion. The wear rate is reported together with its corresponding coefficient of friction.

2.6 Electrochemical analysis

The electrochemical experiment examined the mechanics of electrochemical processes using a typical three-electrode cylindrical glass cell with 100 ml of electrolyte at a temperature of 300 degrees Celsius. The apparatus makes use of three electrodes—a reference electrode, a working electrode, and a counter electrode—to investigate the reaction processes of the working metals or alloys. With the help of the data collected by the Autolab data capture system (Autolab model: AuT71791 and PGSTAT 3.0), the rate of corrosion was calculated using the Tafel extrapolation, and the polarization curves were displayed.

Figure 3. Rice husk (RH) particulate

3. Results and discussion

3.1 Morphology analysis of rice husk nanoparticles

The morphology of rice husk, displayed in Figure 4 and Table 5, revealed Si as the predominant element with percentage weight values close to some literature values [25-27]. Other elements, such as aluminum, calcium, magnesium, potassium, as well as chlorine, sulphur, and manganese were present in the composition [28], [29]. This suggests that the compound was mainly in silicate, phosphate, sulphide, and chloride forms. Aluminum and silicon are known for their microbial corrosion resistance properties and excellent strength-to-weight ratio, which makes them very useful for structural applications [30-33]. This is because they are passive, a property that makes them suitable to produce a tightly adherent film on the substrate's surface when exposed to seawater.

Table 5. Chemical composition of rice husk (RH)

Parameters	Values
SiO_2	69.23
Al_2O_3	0.61
Fe_2O_3	11.79
CaO	5.42
MgO	0.17
K_2O	0.44
P_2O_5	1.13
SO_3	1.22
MnO	0.66

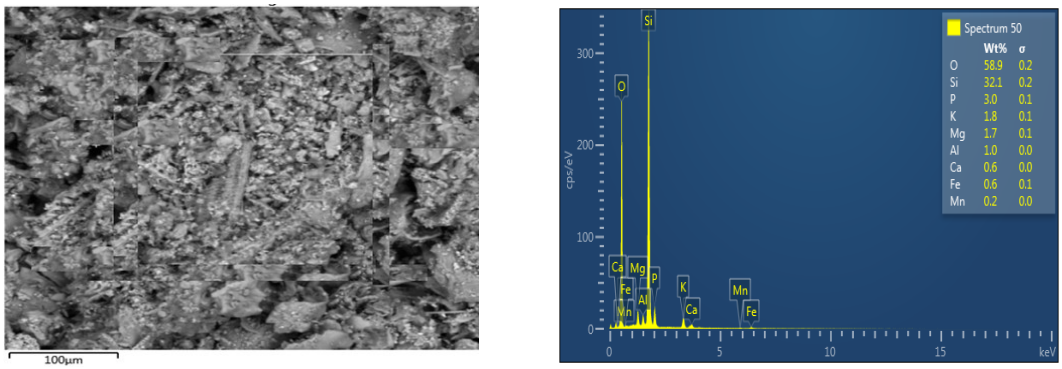

Figure 4. SEM/EDS of rice husk (RH) nano-particulates

3.2 Analysis of a specimen fabricated with rice husk (RH)

This section of the experiment takes into consideration the deposition done using rice husk (RH) particulates. The deposition time and concentration of the particulate were varied. In contrast, other parameters, such as depth of immersion, size of the substrate, distance between cathode and anode, pH, voltage, and the anode used, were kept constant. The variation of the electro-deposition parameters used is shown in Table 6.

Table 6. Variation of the electrodeposition parameters with RH samples

Exp. Run No	Sample Matrix	RH concentration (g/L)	Deposition Time (min)	Voltage (V)
1	Zn-10RH(t25)	10	25	0.5
2	Zn-10RH(t30)	10	30	0.5
3	Zn-15RH(t25)	15	25	0.5
4	Zn-15RH(t30)	15	30	0.5

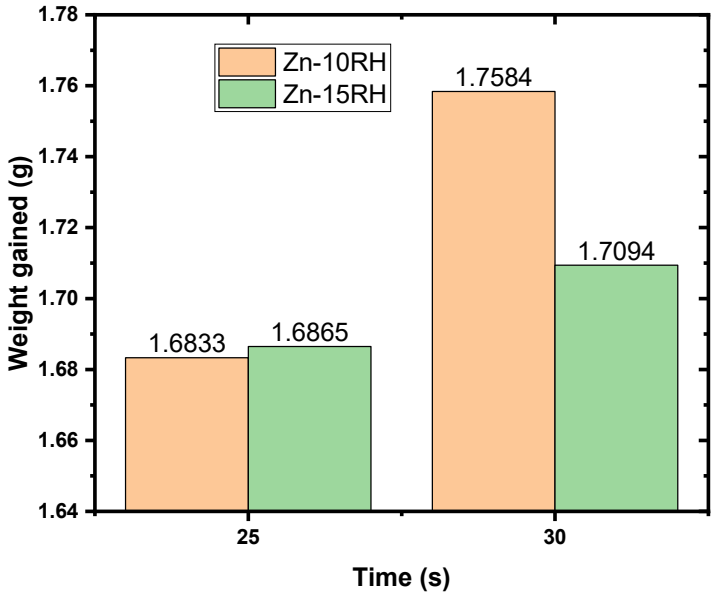

Figure 5. Weight gained at varying deposition time and concentration for RH

The weight gained from the electro-deposition of RH composite coating at varying concentrations (10 and 15 g/l) and deposition time (25 and 30 minutes) is illustrated in Figure 5. The weight of the composite deposits achieved at 0.5 V surprisingly increases as the deposition time, suggesting a

strong adherence of RH at 0.5 V. Also, it indicates that the RH improved the adhesive properties of the coating to some extent. This corresponds with the report of Mohanty et al. [34] and Safavi and Walsh [35]. The studies state that there is a tendency for electrodeposited surfaces to adhere perfectly to a substrate, which is highly influenced by the nature of the additive and the purity of the base particles.

3.3 Coating efficiency of RH deposited samples

The coating efficiency of the RH deposited samples done at constant voltage is shown in Figure 6. Figure 6 indicates that out of the specimens in this section, Zn-15RH(t30) coating had the highest coating efficiency at 53.87%, while Zn-10RH(t25) coatings had the least coating efficiency at 30.16%. This result showed that the coating efficiency increases as the electro-deposition time increases. The impact of time on the coating efficiency of the RH specimen deposited at 0.5 V is relatively significant. This shows that the best coating efficiency was achieved at 30 minutes, which aligns with the weight gained that was discussed, and the coating at 30 minutes is the most stable. However, it was detected that the coating efficiency of the specimen deposited with Zn-RH fell below the standard range of 90-98%. This could be due to low solid/resin content or high solid/resin content, pH imbalances, bath deviation, contamination, improper temperature, inadequate agitation, and improper surface preparation of the specimen. By methodically controlling these parameters and implementing a robust process management system, it is possible to achieve a standard range of coating efficiency for many applications. The standard range of coating efficiency is 90-98 % particularly for metals like copper, nickel, and zinc, by their respective high-performance plating bath. This standard range was established by some specific organizations, like ASTM and ISO, for all electroplating systems. This standard represents the optimum performance for making a conventional well-maintained plating bath where metal deposition is the dominant cathodic reaction. A low coating efficiency could also indicate that a significant portion of the electrical energy is consumed by a side reaction at the cathode rather than the desired metal deposition, which has a detrimental effect on the coating quality.

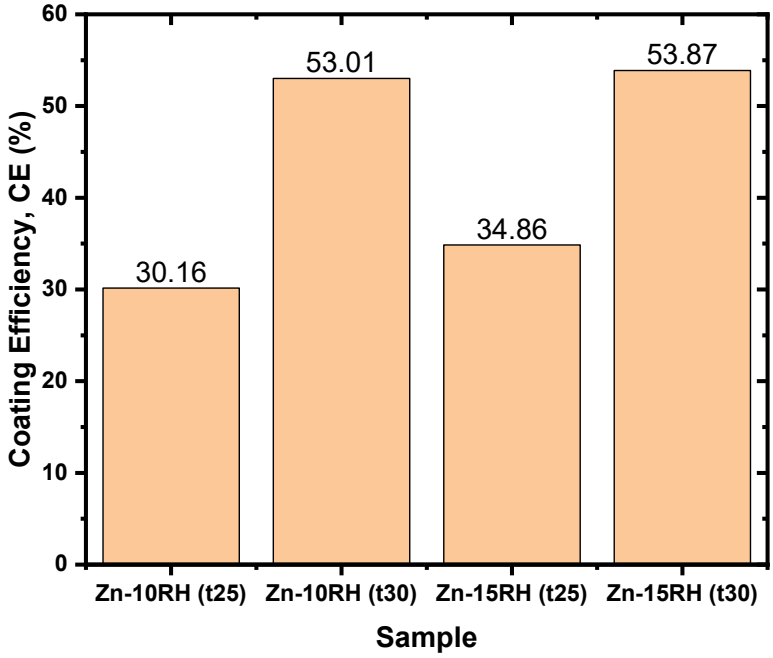

Figure 6. Coating efficiency of RH composite coating at 0.5 V

3.4 Electrochemical behaviour (polarization) of RH deposited samples

Figure 7 shows Tafel curves for RH composite coatings against the control specimen. It can be observed that the corrosion potentials of the deposited Zn-15RH(t30) shifted towards the more negative region, significantly polarized passively. The position of the control specimen (CP) sample compared with the coated specimens signifies that the CP is more susceptible to crevice and pitting corrosion. Similarly, the position of the coated specimens with lesser corrosion potential shows that Zn-15RH composite coatings predominantly protected the cathodic region in the saline environment. This suggests that such a coating can be primarily used for cathodic protection in such a medium; meanwhile, the anodic region will not be left unprotected. This is because the adhesion behavior of the Zn-15RH was strong enough to resist the deterioration of the substrate to some extent and reduce the formation of oxides on the sample when exposed to a salt environment. Such a protective reaction is similar to the findings of [4], [36], and [37] when Zn-Al-SnO_2/TiO_2 functional coating was used on A36 mild steel.

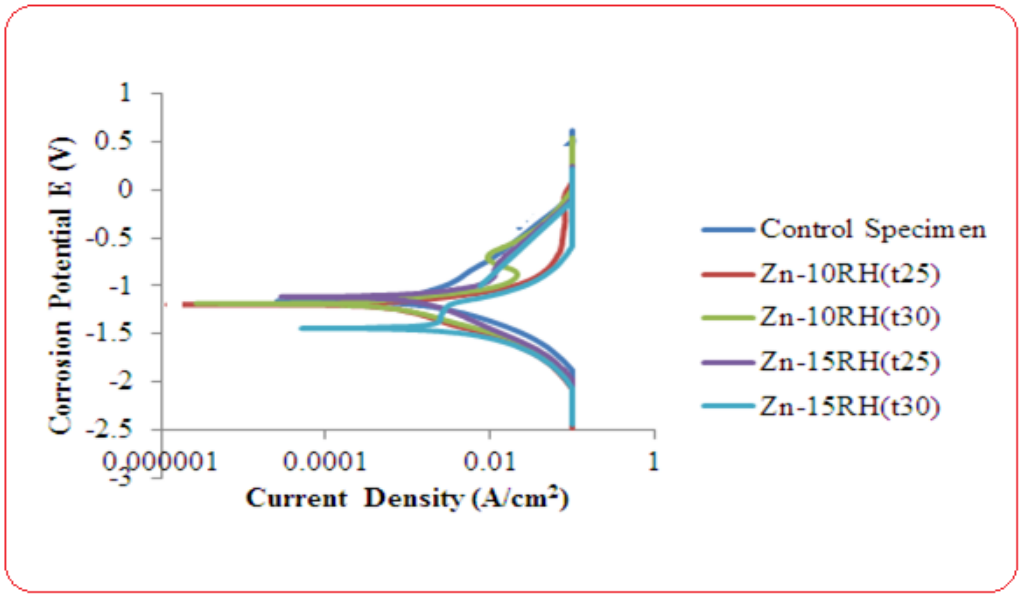

Figure 7. Linear polarization curve for Zn-RH composite coatings at 0.5 V

Table 7 shows the data obtained from polarization measurement for the RH composite coating, which was done at 0.5 V and exposed to a simulated marine (salt water) environment. It was revealed that the coating done for 30 minutes, Zn-15RH(t30), had the highest polarization resistance of 89.275 Ω, Zn-10RH(t30) had the lowest current density and lowest corrosion rate of 0.0001214 A/cm^2 and 1.4107 mm/year, respectively. It can be observed from this table that the rate of corrosion of RH reduced with deposition time and followed the same trend as polarization potential in the reverse order. Such a steady and general reduction in corrosion rate as against the CP sample can be attributed to the adhesion due to the relatively good interfacial bonding of the RH composite coating on the substrate. The potentiodynamic polarization data showed that the polarization resistance increased with electrodeposition time, while the current density and the corrosion rate decreased with electrodeposition time.

The OCP versus time plot shown in Figure 8 indicates that the potential of the RH-coated samples produced at 0.5 V shifted significantly towards the negative scale, confirming the efficacy of the coating as a cathodic protection means. Zn-15RH(t25) and Zn-15RH(t30) coated specimens were able to attain steady state potentials within the first 3 seconds of immersion into the seawater due to the near-zero slope lines observed, which agrees with other findings [38-43]. The coatings were

highly stable up to 120 seconds of immersion. The potentials of the four coatings overlap as they are very close to each other. This trend shows that at 0.5 V, the stability of the coating and its corrosion rate are not really influenced by the deposition time of the coating, but more by the nature of the additive used in the coating.

Table 7. Potentiodynamic polarization of Zn-RH specimen

Specimen Number	Specimen Matrix	Corrosion Potential, E_{corr} (V)	Current density, j_{corr} (A/cm^2)	Corrosion rate, Cr (mm/yr)	Polarization resistance, Pr (Ω)
	Control specimen	-1.1591	0.00072828	8.4626	41.184
1	Zn-10RH(t25)	-1.1965	0.00031351	3.643	59.027
2	Zn-10RH(t30)	-1.1837	0.0001214	1.4107	87.653
3	Zn-15RH(t25)	-1.1147	0.00012648	1.4697	63.227
4	Zn-15RH(t30)	-1.4423	0.00014419	1.6755	89.275

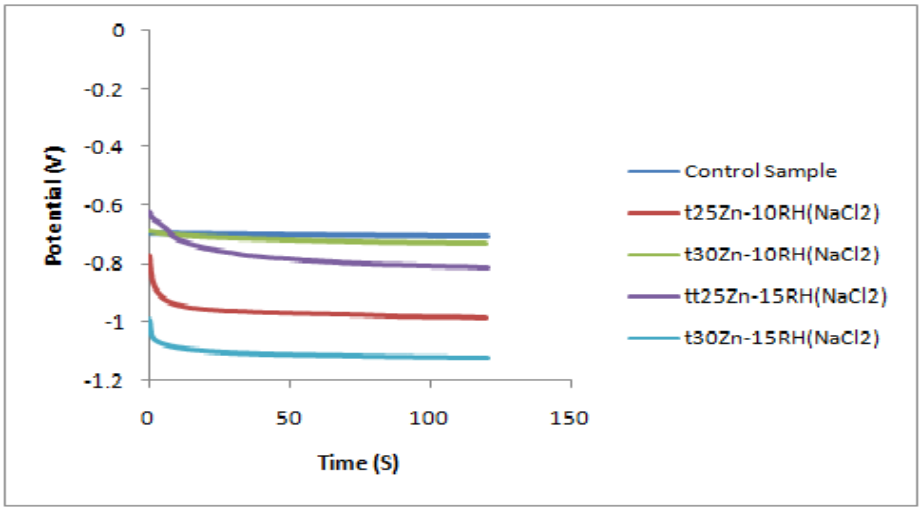

Figure 8. OCP versus time or the Zn-RH composite coatings

3.5 Microstructural characterization of Zn-RH deposited samples

The microstructural features of the thin films obtained from selected Zn-RH composite coating from scanning electron microscopy/Energy Dispersive Spectroscopy (SEM/EDS) at a constant voltage of 0.5 V are shown in Figure 9(a) – (d), respectively, for Zn-10RH(t25), Zn-10RH(t30), Zn-15RH(t25), and Zn-15RH(t30). These micrographs showed layers of coating compared with the micrograph obtained earlier from the control specimen (CS). By critically examining these micrographs, it can be observed that they all show some level of uniform dispersion of the particulates. This suggests that good precipitation and absorption of particulates lead to good adhesion and deposits that are more stable. Zn-15RH(t25) and Zn-15RH(t30), as shown in (Figure 9 (c) and (d)), possess finer grains than Zn-10RH(t25) and Zn-10RH(t30). Figure 9 (a) and (b) validate the findings, which verified that at higher concentrations, there is a tendency to have fine adhesion. This could result in uniform crystal growth [30]. Nevertheless, a few parts of the ferrite were still exposed as the coating did not adhere to those parts. Thus, this makes the coated samples susceptible to a level of marine fouling and corrosion [42-44].

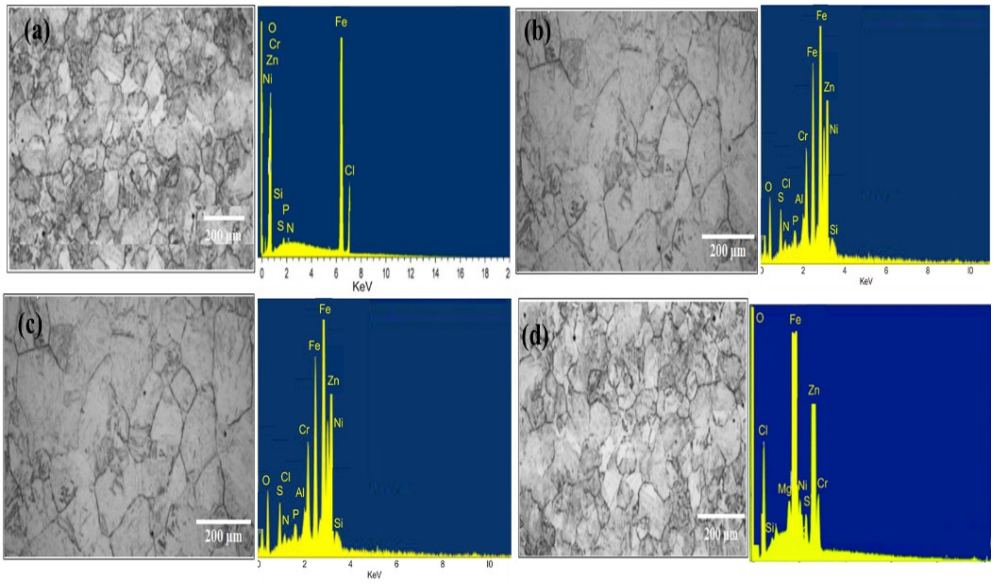

Figure 9. SEM/EDS micrograph of (a) Zn-10RH (t25), (b) Zn-10RH (t30), (c) Zn-15RH (t25), and (d) Zn-15RH (t30) at constant voltage

3.6 XRD Analysis of Zn-RH Composite Coating

Phase identification of Zn-RH composite coating at a constant voltage of 0.5 V was carried out by means of X-ray diffraction analysis. The XRD spectra for samples of Zn-RH composite coating deposited at varying concentrations and times are displayed in Figure 10 (a)-(b). The peaks of ZnAlSi, $ZnSiO_2$, AlO_3, and ZnSi were noted in the spectrum obtained with Zn-RH composite coating. The presence of an intermetallic phase was displayed in the X-ray diffraction obtained. This established that the composition elements and the compounds that constituted the rice husks (RH) were deposited on the substrate.

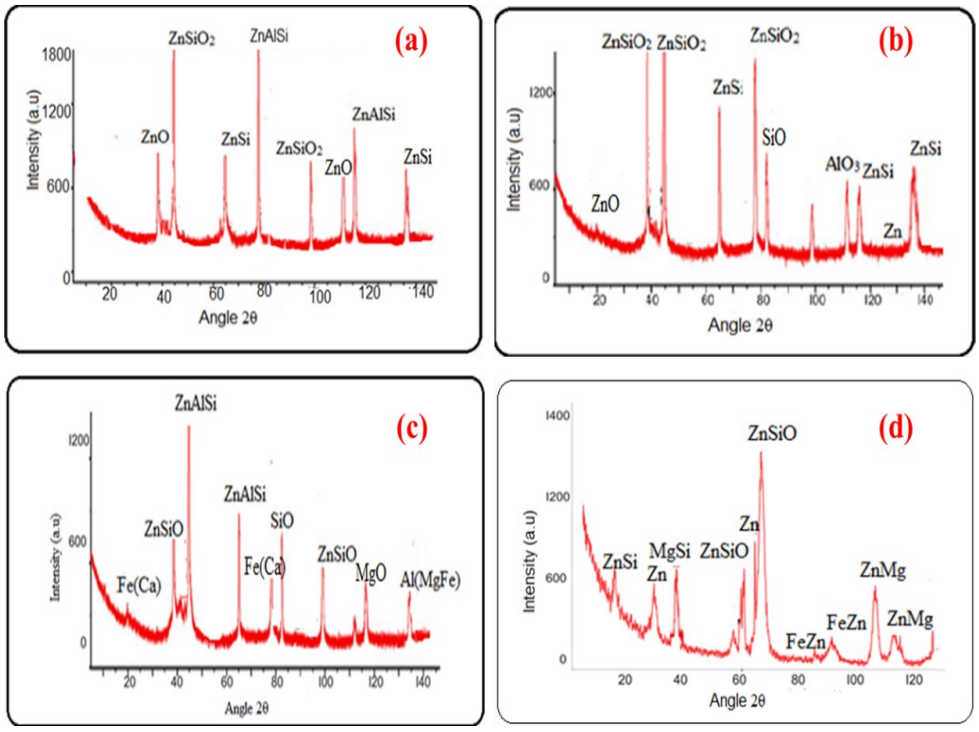

Figure 10. XRD spectra of (a) Zn-10RH (t25), (b) Zn-10RH (t30), (c) Zn-15RH (t25), and (d) Zn-15RH (t30) at constant voltage

3.7 Hardness properties of Zn-RH deposited samples

Table 8 displays the average microhardness data for Zn-RH composite thin film coatings. Carefully observing the deposited materials, Zn-15 RH(t30) gave a better improvement. The hardness increases from 85.82 HV for the control specimen to 288.37 HV for the deposited composites, as shown in Figure 11. All of the samples' hardness profiles exhibit a noticeable average rise, with Zn-10RH(t25) having the lowest average hardness among the matrices at 189.84 HV. The results of hardness obtained imply that the improvement in hardness generally doubles the micro-hardness of the control specimen. This improvement is attributed to the formation of an adhesive mechanism of the alloy coating on the working specimen. The micro hardness of the electrodeposited alloys depends on so many factors, such as the electrolyte and the condition of the operative [35, 45-47]. The microstructure developed in coatings is influenced by metallurgical processing parameters like grain size, which is crucial to the formation of surface hardness [48], [49], as evidenced by the most improved Zn-RH composites deposited at 0.5 V.

Table 8. Hardness data for Zn-RH deposited samples at constant voltage

Hardness Depth (HV)	Control specimen	Zn-10RH(t25)	Zn-10RH(t30)	Zn-15RH(t25)	Zn-15RH(t30)
25	69.12	224.71	275.82	288.41	292.22
30	69.88	240.62	265.22	272.08	284.12
35	70.18	212.62	279.12	292.02	295.02
40	72.28	208.32	275.34	286.32	288.22
45	83.28	222.31	268.42	294.24	272.83
50	73.81	230.44	286.60	284.48	298.40
Average	**85.82**	**189.84**	**275.09**	**286.26**	**288.37**

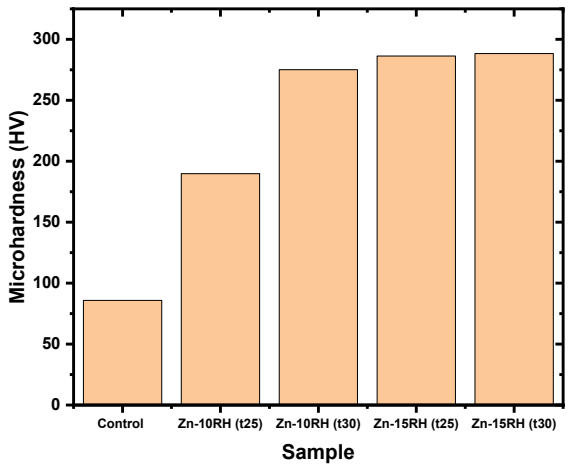

Figure 11. Hardness behaviour of Zn-RH composite coating at 0.5 V

3.8 Wear behaviour and coefficient of friction of Zn-RH coatings

Figure 12 revealed the tribological behavior of complete wear loss of all the matrix compositions and the control specimen samples. The result obtained shows that the wear resistance of the dual anode electrolytic co-deposition composite developed was excellent. The cumulative wear loss is higher for the control specimen. It is evident that the incorporation of RH particulate in the Zn matrix improves the plastic deformation resistance and reduces wear volume loss. Considering the

deposition time and the concentration of the particulate, Zn-10RH(t25) matrix at 25 minutes and 10 g/L produced an excellent wear resistance among composites fabricated at a constant voltage of 0.5 V. The moderate doping of particles increases wear life, which supports the performance of Zn-10RH(t25) [50]. Excessive particles on a Zn matrix film, on the other hand, severely reduce tribological resistance due to phase separation. In general, the ability to produce a functional coating with outstanding wear performance is not a function of excessively injected particles, but instead of a precise modifier that can improve adhesion and tribological properties of the thin film on the substrate, hence increasing wear resistance [51], [52]. In general, all composite thin film coatings are geometrically adequate over the control specimen [53], [54]. A 0.56 coefficient of friction value recorded by the control specimen falls within the range (0.3-0.6) of general values given for ASTM mild steel.

Also, the coefficient of friction was reported alongside the wear rate to observe the friction and the tribological behaviour qualitatively. Zn-10RH(t25) has the highest coefficient of friction value from the series of Zn-RH composite coating against the control specimen (CS) under non-lubricated conditions and at ambient conditions. When compared to other composite coatings at constant voltage, Zn-10RH(t25) showed a low coefficient of friction and wear rate. It is therefore more necessary to explain at this point that the composite thin film coating has a lower friction coefficient due to various crystal sizes aligned within the Zn-matrix contact. Changes in the microstructure of thin films are related to the reduced behaviour [55-57]. It was observed that the wear rate decreases with hardness in accordance with Archard's theory [58-60]. The results in this work are comparable to the existing work, which shows the consistency of the work.

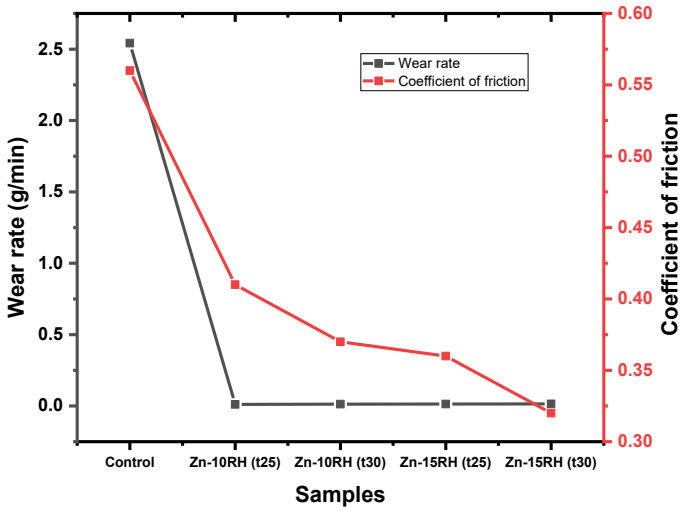

Figure 12. Variation of wear rate and coefficient of friction of Zn-RH deposition samples

4. Conclusion

Dual electro-deposition of Zinc-based RH composite coatings on A36 mild steel at a constant voltage of 0.5 V was carried out. The study investigated the effects of the electrodeposited composite coatings on the corrosion behaviour of the steel in a salt environment. Also, the present research examined the hardness and wear behaviour of the coatings on the steel specimen. The following are the conclusions derived from the study.

a. The morphology of the rice husk revealed the predominance of the Si element in the rice husk. The rice husk nanoparticle is suitable for producing an adherent film on the substrate's surface.

b. The weight gain of the electro-deposition coating of the RH composite with Zinc increased with varying concentrations and deposition time.
c. The highest coating efficiency of 53.87% was obtained for sample Zn-15RH(t30), and the least coating efficiency was 30.16% at Zn-10RH(t25).
d. The Tafel polarization result showed that Zn-15RH composite coatings predominantly protected the substrates in the saline environment. Zn-10RH samples had the lowest corrosion rate of 0.0001214 A/cm^2.
e. The hardness improved from the control (85.82 HV) to the sample Zn-15RH(t30) (288.37 HV). The improvement observed is linked to the formation of the adhesive mechanism of the alloy coating on the substrate.
f. The coefficient of friction and wear rate of the samples reduced with increased concentration and deposition time. Hence, the composite thin film coating has a lower friction coefficient due to various crystal sizes aligned with the Zn-matrix.

Author's declaration

Author contribution

Samuel A. Ajayi: Conceptualization, Methodology, Validation, data curation, original draft; **Peter Onu**: Review and Editing; **Peter P. Ikubanni and Timothy A. Adekanye:** Validation, Review and Editing; **Abideen T. Oyewo**: Review and Editing; **Olufemi Ajide**: Supervision and Validation.

Funding statement

This research received no specific grant from any funding agency in the public, commercial, or not-for-profit sectors.

Data availability

The raw data of this study will be made available upon reasonable request.

Acknowledgements

The authors are grateful for the conducive environment provided by Bowen University to carry out this study.

Competing interest

There are no conflicts of interest in this research.

Ethical clearance

This research does not involve humans as subjects.

AI statement

This article is the original work of the authors without using AI tools for writing sentences and/or creating/editing tables and figures in this manuscript.

Publisher's and Journal's note

Universitas Negeri Padang as the publisher, and Editor of Teknomekanik state that there is no conflict of interest towards this article publication.

References

[1] U. Kumar Debnath, M. Asaduzzaman Chowdhury, N. Hossain, M. Aminul Islam, and D. N. Muhammad, "Solid particle erosion behavior of Graphene/SiC/Al2O3/TiO2 coated Kevlar/Epoxy composite materials," *Results Chem*, vol. 7, p. 101396, 2024, https://doi.org/10.1016/j.rechem.2024.101396

[2] P. Rani and S. K. K. Pasha, "A study of EMI shielding efficiency, dielectric, and impedance properties of polymer nanocomposites reinforced with Graphene nanoplatelets, montmorillonite, and copper oxide nanoparticles," *Poly Plastics Technol Mater*, vol. 63, no. 16, pp. 2258–2275, 2024, https://doi.org/10.1080/25740881.2024.2369680

[3] M. Chanda, A. Kar, and S. Banerjee, "Comparison of hardness by electrolytic and electroless deposition of nickel on aluminium," *IOP Conf Series: Mater Sci Eng*, vol. 1316, p. 012012, 2024, https://doi.org/10.1088/1757-899X/1316/1/012012

[4] O. S. I. Fayomi, A. A. Daniyan, A. P. I. Popoola, O. Patrick, and O. R. Olatunji, "Investigation on the functionally graded properties of Zn–6MgO–12MnO2 composite coating fabricated by dual anode electrolytic deposition technique," *J Bio Tribo Corros*, vol. 5, p. 102, 2019, https://doi.org/10.1007/s40735-019-0295-8

[5] S. Mei *et al.*, "Optimization of Ni-B-Mo electroless coating on GCr15 steel: Effects of main salt concentration and deposition time," *Materials*, vol. 18, no. 9, p. 1981, 2025, https://doi.org/10.3390/MA18091981

[6] F. T. Z. Toma, M. S. Rahman, and K. H. Maria, "A review of recent advances in ZnO nanostructured thin films by various deposition techniques," *Discov Mater*, vol. 5, p. 60, 2025, https://doi.org/10.1007/S43939-025-00201-1

[7] M. Abdulwahab, O. S. I. Fayomi, and A. P. I. Popoola, "Structural evolution, thermomechanical recrystallization and electrochemical corrosion properties of Ni-Cu-Mg amorphous coating on mild steel fabricated by dual-anode electrolytic processing," *Appl Surf Sci*, vol. 375, pp. 162–168, 2016, https://doi.org/10.1016/j.apsusc.2016.03.075

[8] H. M. Saleh and A. I. Hassan, "Synthesis and characterization of nanomaterials for application in cost-effective electrochemical devices," *Sustainability*, vol. 15, no. 14, p. 10891, 2023, https://doi.org/10.3390/SU151410891

[9] A. W. B. Santosa, A. A. Alkhudry, U. Budiarto, E. S. Hadi, and A. Trimulyono, "Analysis of the effect of voltage and zinc plating duration on low carbon steel A36 by electroplating process on corrosion rate," *Int J Marine Eng Innov Res*, vol. 9, no. 2, 2024, https://doi.org/10.12962/J25481479.v9i2.20262

[10] S. Awasthi, B. Prior Palomero, A. Srivastava, S. Selvaraj, and S. K. Pandey, "Nanodiamond-structured zinc composite coatings with strong bonding and high load-bearing capacity," *Nanoscale Adv*, vol. 6, no. 3, pp. 1001–1010, 2024, https://doi.org/10.1039/D3NA00809F

[11] P. Sahoo, S. K. Das, and J. Paulo Davim, "Surface finish coatings," *Comprehen Mater Finishing*, vol. 3, pp. 38–55, 2017, https://doi.org/10.1016/B978-0-12-803581-8.09167-0

[12] P. P. Kulkarni, B. Siddeswarappa, and K. S. H. Kumar, "A Survey on effect of agro waste ash as reinforcement on aluminium base metal matrix composites," *Open J Compos Mater*, vol. 9, no. 3, pp. 312–326, 2019, https://doi.org/10.4236/OJCM.2019.93019

[13] H. I. Akbar, E. Surojo, D. Ariawan, G. A. Putra, and R. T. Wibowo, "Effect of reinforcement material on the properties of manufactured aluminium matrix composite using stir casting route.," *Procedia Structural Integrity*, vol. 27, pp. 62–68, 2020. https://doi.org/10.1016/j.prostr.2020.07.009

[14] F. Ben and P. A. Olubambi, "Agro waste reinforcement of metal matrix composites, a veritable sustainable engineering achievement, or an effort in futility? A critical review," *Mater Res Express*, vol. 11, no. 6, p. 062004, 2024, https://doi.org/10.1088/2053-1591/AD5642

[15] N. S. Ebenezer, B. Vinod, and H. S. Jagadesh, "Corrosion behaviour of bamboo leaf ash-reinforced nickel surface-deposited aluminium metal matrix composites," *J Bio Tribo Corros*, vol. 7, p. 72, 2021, https://doi.org/10.1007/s40735-021-00510-x

[16] T. Hasan, M. Wadud, M. H. Niaz, M. K. Uddin, and M. S. Islam, "Fabrication and characterization of rice husk ash reinforced aluminium matrix composite," *Malaysian J Compos Sci Manuf*, vol. 14, no. 1, pp. 34–43, 2024, https://doi.org/10.37934/mjcsm.14.1.3443

[17] O. C. Olorunyolemi, O. A. Ogunsanya, A. A. Akinwande, O. A. Balogun, and M. Saravana Kumar, "Enhanced mechanical behaviour and grain characteristics of aluminium matrix composites by cold rolling and reinforcement addition (rice husk ash and coal fly ash)," *Proceed Inst Mech Eng, Part E: J Process Mech Eng*, vol. 237, no. 5, pp. 1709–1721, 2023, https://doi.org/10.1177/09544089221124462

[18] A. Ranjan, H. Kumar, L. Nagdeve, A. Mishra, G. K. Gaurav, and J. J. Klemeš, "Mechanical properties of rice husk ash, an environmental pollutant, based composites: A step towards sustainable hybrid composites," *Energy Sources, Part A: Recov Utiliz Environ Effects*, vol. 44, no. 4, pp. 9584–9602, 2022, https://doi.org/10.1080/15567036.2022.2130476

[19] S. Tiwari and M. K. Pradhan, "Effect of rice husk ash on properties of aluminium alloys: A review," *Mater Today: Proceed*, vol. 4, no. 2, pp. 486–495, 2017, https://doi.org/10.1016/J.matpr.2017.01.049

[20] S.-C. Shi, X.-N. Tsai, and D. Rahmadiawan, "Enhancing the tribological performance of hydroxylpropyl methylcellulose composite coatings through nano-sized metal and oxide additives: A comparative study," *Surf Coating Technol*, vol. 483, p. 130712, 2024, https://doi.org/10.1016/j.surfcoat.2024.130712

[21] F. U. Whyte, A. L. Mgboh, G. M. Whyte, and P. O. Offor, "Microstructural and corrosion studies of Ni-P/rice husk ash composite coatings on mild steel," *J Nano Mater Sci Res*, vol. 1, pp. 76–82, 2022. https://journals.nanotechunn.com/jnmsr/article/view/9

[22] C. C. Daniel-Mkpume, D. O. N. Obikwelu, and V. S. Aigbodion, "Anti-wear and hardness values of functional value-added Zn-ZnO-rice husk ash composite coating of mild steel," *J Comp Adv Mater*, vol. 31, no. 1, pp. 27–32, 2021, https://doi.org/10.18280/rcma.310104

[23] S. A. Ajayi, P. Onu, N. S. Madonsela, A. Pradhan, O. O. Ajide, and O. O. Oluwole, "A dual-anode electrolytic codeposition approach to enhance A36 steel properties with Zn-13, rice husk and white clay coatings," *Mater Des Process Comm*, vol. 25, no. 1, p. 5415075, 2025, https://doi.org/10.1155/mdp2/5415075

[24] C. M. P. Kumar, M. P. G. Chandrashekarappa, R. M. Kulkarni, D. Y. Pimenov, and K. Giasin, "The effect of Zn and Zn-WO3 composites nano-coatings deposition on hardness and corrosion resistance in steel substrate," *Mater*, vol. 14, no. 9, p. 2253, 2021, https://doi.org/10.3390/ma14092253

[25] N. T. Nguyen *et al.*, "The extraction of lignocelluloses and silica from rice husk using a single biorefinery process and their characteristics," *J Indus Eng Chem*, vol. 108, pp. 150–158, 2022, https://doi.org/10.1016/j.jiec.2021.12.032

[26] Y. Zou and Y. Yang, "Chapter 9 - Rice husk, rice husk ash and their applications," in *Rice bran and rice bran oil*, L.-Z. Cheong and X. Xu, Eds., AOCS Press, 2019, pp. 207–246. https://doi.org/10.1016/B978-0-12-812828-2.00009-3

[27] T.-H. Liou, "Preparation and characterization of nano-structured silica from rice husk," *Mater Sci Eng: A*, vol. 364, no. 1–2, p. 3130323, 2004, https://doi.org/10.1016/j.msea.2003.08.045

[28] R. Kathpalia and S. C. Bhatla, "Plant Mineral Nutrition," in *Plant Physiology, Development and Metabolism*, Singapore, Singapore: Springer, 2018, pp. 37–81. https://doi.org/10.1007/978-981-13-2023-1_2

[29] E. A. Kirkby, "Introduction, definition, and classification of nutrients," in *Marschner's Mineral Nutrition of Plants*, Elsevier, 2023, pp. 3–9. https://doi.org/10.1016/B978-0-12-819773-8.00016-2

[30] L. Qiu, S. Dong, A. Ashour, and B. Han, "Antimicrobial concrete for smart and durable infrastructures: A review," *Construct Building Mater*, vol. 260, p. 120456, 2020, https://doi.org/10.1016/j.conbuildmat.2020.120456

[31] Y. Lekbach *et al.*, "Chapter Five - Microbial corrosion of metals: The corrosion microbiome," *Adv Microbial Physiol*, vol. 78, pp. 317–390, 2021, https://doi.org/10.1016/bs.ampbs.2021.01.002

[32] P. Rao and L. Mulky, "Microbially influenced corrosion and its control measures: A critical review," *J Bio Tribo Corros*, vol. 9, p. 57, 2023, https://doi.org/10.1007/s40735-023-00772-7

[33] V. Jamwal, A. Mittal, and A. Dhaundiyal, "Valorization of agro-industrial waste in composite films for sustainable packaging applications," *Mater Today: Proceed*, vol. 113, pp. 94–100, 2024, https://doi.org/10.1016/J.matpr.2023.08.042

[34] U. S. Mohanty, B. C. Tripathy, P. Singh, A. Keshavarz, and S. Iglauer, "Roles of organic and inorganic additives on the surface quality, morphology, and polarization behavior during nickel electrodeposition from various baths: A review," *J Appl Electrochem*, vol. 49, pp. 847–870, 2019, https://doi.org/10.1007/s10800-019-01335-w

[35] M. S. Safavi and F. C. Walsh, "Electrodeposited Co-P alloy and composite coatings: A review of progress towards replacement of conventional hard chromium deposits," *Surf Coatings Technol*, vol. 422, p. 127564, 2021, https://doi.org/10.1016/j.surfcoat.2021.127564

[36] O. S. I. Fayomi and I. G. Akande, "orrosion mitigation of aluminium in 3.65% NaCl medium using hexamine," *J Bio Tribo Corros*, vol. 5, p. 23, 2019, https://doi.org/10.1007/s40735-018-0214-4

[37] O. S. I. Fayomi, A. P. I. Popoola, and V. S. Aigbodion, "Effect of thermal treatment on the interfacial reaction, microstructural and mechanical properties of Zn–Al–SnO2/TiO2 functional coating alloys," *J Alloys Compds*, vol. 617, pp. 455–463, 2014, https://doi.org/10.1016/j.jallcom.2014.07.141

[38] P. P. Ikubanni, M. Oki, A. A. Adediran, S. A. Akintola, and A. A. Adeleke, "Scanning and transmission electron microscopy examinations of composite hybrid chromate and chromate phosphate conversion coatings exposed in hot 100% relative humidity environments," *Hybrid Advances*, vol. 3, no. February, p. 100067, 2023, https://doi.org/10.1016/j.hybadv.2023.100067

[39] P. P. Ikubanni *et al.*, "Application of conversion coatings on aluminium matrix composites for corrosion protection," *Portugaliae Electrochimica Acta*, vol. 43, no. 3, pp. 165–176, 2025, https://doi.org/10.4152/pea.2025430302

[40] M. Oki, P. P. Ikubanni, A. A. Adediran, O. S. Adesina, and A. A. Adeleke, "Electrochemical Evaluation of Corrosion Control by Composite Hybrid Vanadate Conversion Coatings on 6061 Al," *Portugaliae Electrochimica Acta*, vol. 43, pp. 309–322, 2025, https://doi.org/doi.org/10.4152/pea.2025430504

[41] E. Hadjittofis, M. A. Isbell, V. Karde, S. Varghese, C. Ghoroi, and J. Y. Y. Heng, "Influences of crystal anisotropy in pharmaceutical process development," *Pharm res*, vol. 35, p. 100, 2018, https://doi.org/, https://doi.org/10.1007/s11095-018-2374-9

[42] M. Carve, A. Scardino, and J. Shimeta, "Effects of surface texture and interrelated properties on marine biofouling: A systematic review," *J Bioadhes Biofilm Res*, vol. 35, no. 6, pp. 597–617, 2019, https://doi.org/10.1080/08927014.2019.1636036

[43] A. K. Halvey, B. Macdonald, A. Dhyani, and A. Tuteja, "Design of surfaces for controlling hard and soft fouling," *Philoso Trans R Soc A*, vol. 377, p. 20180266, 2019, https://doi.org/10.1098/rsta.2018.0266

[44] G. Gizer, U. Önal, M. Ram, and N. Şahiner, "Biofouling and mitigation methods: A review," *Biointerf Res Appl Chem*, vol. 13, no. 2, pp. 1–25, 2023, https://doi.org/10.33263/BRAIC132.185

[45] J. G. Costa, J. M. Costa, and A. F. Almeida Neto, "Progress on electrodeposition of metals and alloys using ionic liquids as electrolytes," *Metals (Basel)*, vol. 12, no. 12, p. 2095, 2022, https://doi.org/10.3390/met12122095

[46] I. Khazi and U. Mescheder, "Micromechanical properties of anomalously electrodeposited nanocrystalline Nickel-Cobalt alloys: A review," *Mater Res Express*, vol. 6, p. 082001, 2019, https://doi.org/10.1088/2053-1591/ab1bb0

[47] A. Lelevic and F. C. Walsh, "Electrodeposition of NiP alloy coatings: A review," *Surf Coatings Technol*, vol. 369, pp. 198–220, 2019, https://doi.org/10.1016/j.surfcoat.2019.03.055

[48] P. Sang *et al.*, "Particle size-dependent microstructure, hardness, and electrochemical corrosion behavior of atmospheric plasma sprayed NiCrBSi coatings," *Metals (Basel)*, vol. 9, p. 1342, 2022, https://doi.org/10.3390/met9121342

[49] P. Zhang *et al.*, "Recent progress on the microstructure and properties of high entropy alloy coatings prepared by laser processing technology: A review," *J Manufac Process*, vol. 76, pp. 397–411, 2022, https://doi.org/10.1016/j.jmapro.2022.02.006

[50] D. Van Hoang, A. Tuan Thanh Pham, T. Huu Nguyen, T. Bach Phan, and V. Cao Tran, "Impact of Zn doping on the structural properties and thermoelectric performance of CuCr 0.85 Mg (0.15-x) Zn x O 2 (x ≤ 0.05) delafossite materials," *Adv Compos Mater*, vol. 33, no. 5, pp. 778–793, 2024, https://doi.org/10.1080/09243046.2023.2300587

[51] B. Warcholinski and A. Gilewicz, "Multilayer coatings on tools for woodworking," *Wear*, vol. 271, no. 11–12, pp. 2812–2820, 2011, https://doi.org/10.1016/j.wear.2011.05.048

[52] J. Yu *et al.*, "Tribological properties of hard TiB2 thin films prepared at low temperatures using HiPIMS," *Coatings*, vol. 14, p. 492, 2024, https://doi.org/10.3390/coatings14040492

[53] M. F. Ismail, M. A. Islam, B. Khorshidi, A. Tehrani-Bagha, and M. Sadrzadeh, "Surface characterization of thin-film composite membranes using contact angle technique: Review of quantification strategies and applications," *Adv. Colloid Interface Sci*, vol. 299, p. 102524, 2022, https://doi.org/10.1016/j.cis.2021.102524

[54] M. Sathish, N. Radhika, and B. Saleh, "A critical review on functionally graded coatings: Methods, properties, and challenges," *Composites Part B: Eng*, vol. 225, p. 109278, 2021, https://doi.org/https://doi.org/10.1016/j.compositesb.2021.109278

[55] G. Abadias *et al.*, "Stress in thin films and coatings: Current status, challenges, and prospects," *J Vacuum Sci Technol A*, vol. 36, no. 2, 2018, https://doi.org/10.1116/1.5011790.hal-01942286

[56] A. Barranco, A. Borras, A. R. Gonzalez-Elipe, and A. Palmero, "Perspectives on oblique angle deposition of thin films: From fundamentals to devices," *Progress Mater Sci*, vol. 76, pp. 59–153, 2016, https://doi.org/10.1016/j.pmatsci.2015.06.003

[57] R. Nasrin, H. Kabir, H. Akter, and A. H. Bhuiyan, "Effect of film thickness on topographic, microstructural, optical and dielectric behaviour of PPMBA thin films," *Results Phys*, vol. 19, p. 103357, 2020, https://doi.org/10.1016/j.rinp.2020.103357

[58] B. Liu, S. Bruni, and R. Lewis, "Numerical calculation of wear in rolling contact based on the Archard equation: Effect of contact parameters and consideration of uncertainties," *Wear*, vol. 490–491, p. 204188, 2022, https://doi.org/10.1016/j.wear.2021.204188

[59] M. H. Nazir, Z. A. Khan, A. Saeed, V. Bakolas, W. Braun, and R. Bajwa, "Experimental analysis and modelling for reciprocating wear behaviour of nanocomposite coatings," *Wear*, vol. 416, pp. 89–102, 2018, https://doi.org/10.1016/j.wear.2018.09.011

[60] A. Shebani and C. Pislaru, "Wear measuring and wear modelling based on Archard, ASTM, and neural network models," *Int J Mech Aerosp Indus Mechatron Eng*, vol. 9, no. 1, pp. 177–182, 2015. https://publications.waset.org/10000683.pdf